Journal of Thermal Analysis and Calorimetry, Vol. 91 (2008) 3, 873–878

HYDRATED GOETHITE NANORODS
Vibration spectral properties, thermal stability, and their potential application in removing cadmium ions

X. Q. Qiu[1], *L. Lv*[1,2], *G.-S. Li*[1], *W. Han*[3], *X.-J. Wang*[2] *and L.-P. Li*[1*]

[1]State Key Structural Chemistry Laboratory, Fuzhou Institute of Research on the Structure of Matter, Graduate School of Chinese Academy of Sciences, Fuzhou 350002, P.R. China
[2]School of Chemistry and Chemical Engineering, Inner Mongolia University, Hohhot 010021, P.R. China
[3]Department of Physics, Jilin University, Changchun 130023, P.R. China

Vibration spectral properties and dehydration behaviors of goethite nanorods with diameters ranging from 13 to 32 nm were investigated using infrared spectroscopy, thermogravimetric analysis, and X-ray diffraction. All goethite nanorods were highly hydrated with physisorbed and chemisorbed water. As the diameters of goethite nanorods increased, the hydroxyl deformation vibration in the *a–b* plane showed a significant blue shift, while the Fe–O vibration in the *a–b* plane shifted to lower frequencies, indicating an enhancement of O–H bond and the ionicity of Fe–O in *a–b* plane. The hydrated goethite nanorods are also proved to be useful in environmental remedy because of their excellent removal ability of heavy metal ions.

Keywords: *dehydration, goethite, infrared spectroscopy, surface structures, thermogravimetric analysis, X-ray diffraction*

Introduction

Iron oxide and oxyhydroxide have attracted extensive technological and scientific attention due to their potential applications in pigments, catalysts, gas sensors, magnetic recording media and so on [1]. Goethite (α-FeOOH), as one of the most common iron oxyhydroxides in nature [2], is frequently used as an important raw material to produce magnetic iron oxide and pigments. It is well known that the thermal transformation of goethite to hematite is a crucial step in further fabricating iron oxides [3]. Many theoretical and experimental investigations have been performed to study the mechanism of this transformation [4]. By spectral investigations, Wolska [5] concluded that goethite is firstly transformed into hydrohematite and then into hematite with increasing temperatures. Özdemir and Dunlop [6] studied the low-temperature dehydration of goethite and found that small amounts of magnetite occurred as the intermediate product during the thermal transformation. Gualtieri *et al.* [7] performed and in-situ study of the goethite–hematite phase transformation by real time synchrotron powder diffraction and demonstrated that an intermediate phase with nonstoichiometric composition (protohematite) formed after the decomposition of goethite. While, Watari *et al.* [8] and Goss [9] concluded that the transformation proceeded via a direct dehydration of goethite to hematite without any intermediate phase.

These results in debate are correlated with the surface hydration of goethite compounds. As is for all nanoscale solids, the sizes and structural properties are highly related with the surface hydration [10]. As a result, thermal stability and surface hydration structure of goethite have great influences on the physical and chemical properties and are directly relevant to the current problems in their applications. Betancur *et al.* [11] studied the effect of water content on the magnetic and structure properties of goethite and concluded that the surface water and excess hydroxyls played the substantial roles in the magnitude of the hyperfine field. Walter *et al.* [4] observed the dependence of the dehydration mechanism on the commercial goethite particle size. Apparently, these inconsistent and confusing results among different research groups mentioned above are owing to the lack of knowledge about the surface hydration structure of goethite.

On the other hand, the surface hydrated structural properties and optical spectra are significantly influenced by the finite size effects. Recent works by Li *et al*. [12, 13] have clearly demonstrated that the surfaces of nanoparticles became highly hydrated with a particle size reduction and the finite size effects were indicated by a systematic shift in the electronic spectra. Several infrared investigations on goethite [14, 15] have established that two broad bands at 3136 and 3415 cm^{-1} are associated with the surface hydroxyl and bulk hydroxyl stretching modes, whereas the bands located at 894 and 796 cm^{-1} are im-

* Author for correspondence: lipingli@fjirsm.ac.cn

1388–6150/$20.00

Akadémiai Kiadó, Budapest, Hungary
Springer, Dordrecht, The Netherlands

portant diagnostic modes of goethite. However, the influence of particle size or the surface hydration layer on the infrared spectrum is not unclear. Herein, we prepared goethite nanorods with different diameters. We systematically studied their size-related vibration and thermal stability properties. We also found that hydrated goethite nanorods can be used to remove the heavy metal Cd^{2+} ions from wastewater.

Experimental

All chemical reagents used in this work were of analytical grade. The detailed synthetic procedures are described as follows: Firstly, 8 g (0.2 mol) of sodium hydroxide was dissolved in 150 mL distilled water. Then, freshly prepared 100 mL of 0.6 M ferrous chloride solution was added drop-wise into the above solution under vigorously stirring. Keeping stirring at room temperature for 3 h, a yellow suspension solution was formed. The precipitate was aged at room temperature for 12 h, then washed fully with distilled water and dried at 40°C for 6 h. The sample thus obtained was named as G-RT. To precisely control the sizes of goethite nanoparticles, the as-prepared yellow suspension solution was transferred to 25 mL Teflon-lined stainless steel autoclaves, sealed and hydrothermally treated at 100, 120, 140, 160, 180, and 200°C for 12 h, respectively. When the formation reactions were completed, autoclaves were cooled naturally to room temperature. The yellow products were harvested by pressure filtration, and washed fully with distilled water until no chloride anions in the supernatant were detected using 1 M $AgNO_3$ solution. The products were then dried at 40°C for 6 h and named as G-100, G-120, G-140, G-160, G-180 and G-200, respectively.

Structural characteristics of the samples were measured by powder X-ray diffraction (XRD) at room temperature on a Rigaku D/MAX25000 diffractometer with a copper target. The average grain sizes (*D*) were calculated from the most intense diffraction peak (110) using the Scherrer formula, $D=0.9\lambda/\beta\cos\theta$, where λ is the X-ray wavelength employed, θ is the diffraction angle of the most intense peak (110) and β is defined as the half-width after subtracting the instrumental broadening. The particle sizes and morphologies of the samples were investigated using transmission electron microscope (TEM) on a JEM-2010 apparatus with an acceleration voltage of 200 kV. The specific surface areas of the goethite nanocrystallines were determined from the nitrogen absorption data at liquid nitrogen temperature using Barrett–Emmett–Teller (BET) technique on a Micromeritics ASAP 2000 Surface Area and Porosity Analyzer. The infrared optical properties were measured using a Perkin-Elmer IR spectrophotometer at a resolution of 4 cm^{-1}. Water contents of the samples were determined using thermogravimetric analysis (TG) at a heating rate of 15°C min^{-1} from room temperature to 900°C in a N_2 atmosphere at a flux of 30 mL min^{-1} and under ambient atmospheric pressure.

The removal capability of low concentration heavy metal ions from wastewater was investigated. Firstly, aqueous solution of Cd^{2+} was prepared from analytical reagent grade $CdNO_3{\cdot}4H_2O$ with a concentration of 0.14 mg L^{-1}. 0.2 g of as-prepared samples were suspended in 200 mL Cd^{2+} solution with magnetically stirring at room temperature. The pH value of the system was set at 6.0±0.5. After staying in air for a given period of time, 10 mL aliquots of the suspension were withdrawn and centrifuged. The concentration of Cd^{2+} in the supernatants was determined by flame atomic absorption spectroscopy using Varian AA-10 spectrophotometer.

Results and discussion

Figure 1 gives the XRD pattern for G-RT sample obtained at room temperature. No impurity peaks associated with β-FeOOH, γ-FeOOH, or α-Fe_2O_3 were observed. All diffraction peaks matched well the standard data for goethite (JCPDS card No. 29-0713), indicating the formation of pure α-FeOOH. All diffraction peaks were broadened, which can be the result of the fine particle size. XRD patterns of the samples after hydrothermal treatments are similar to that of G-RT sample. A slight sharpening of the XRD peaks with increasing the treatment temperature is observed, as shown in inset of Fig. 1, although all diffraction peaks still exhibited a high degree of broadness due to their small particle sizes. By application of the Scherrer formula, the average particle sizes cal-

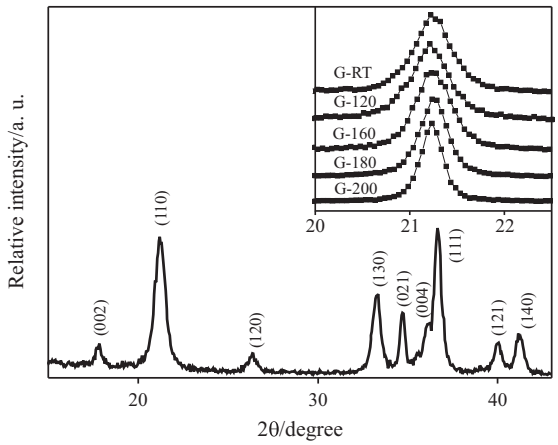

Fig. 1 X-ray diffraction pattern of G-RT sample. Inset represents the enlarged diffraction peak (110) for goethite samples obtained after hydrothermal treatments at given temperatures

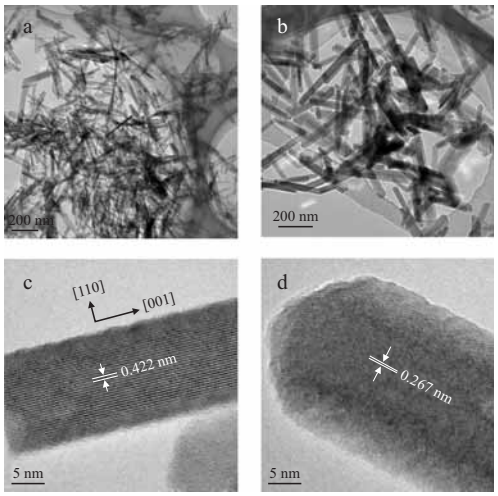

Fig. 2 TEM images of some selected goethite samples a – G-100 and b – G-180, and HRTEM images for c – G-100 and d – G-180

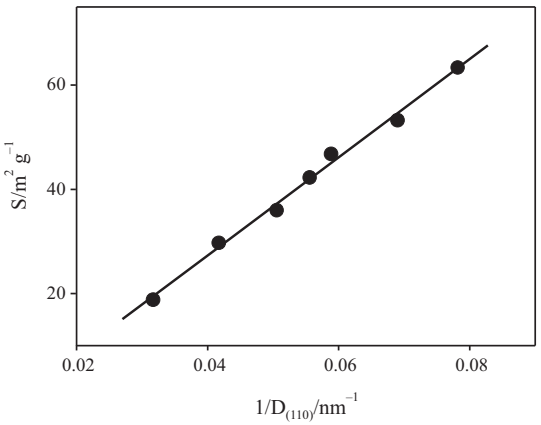

Fig. 3 Relationship between the specific surface areas (*S*) and the diameters (*D*) of goethite nanorods

culated from the most intense diffraction peak (110) are 13, 17, 20, 24 and 32 nm for G-RT, G-120, G-160, G-180 and G-200, respectively.

Morphology of the goethite samples was visualized by TEM measurements. TEM images for G-100 and G-180 are shown in Figs 2a and b. It is seen that all samples consisted of uniformly distributed nanorods with perfectly smooth surfaces. The top end of FeOOH nanorods was acicular. From Fig. 2, it can be found that increasing the hydrothermal treatment temperature did not significantly change the particle shape of goethite. The corresponding high resolution transmission electron microscopy (HRTEM) photos presented in Figs 2c and d clearly showed that the samples are composed of tiny single crystals with high crystallinity, while the amorphous layer or short-range disordering distribution is also seen at surfaces. The interplanar spacing value of the goethite nanorods was about 0.422 nm for G-100 and 0.267 nm for G-180, which are much closer to those of 0.418 nm for (110) plane and 0.269 nm for (130) plane as calculated from XRD. These results indicated that the nanorods grew along the [001] direction (*c*-axis). The average diameter of G-100 nanorods was about 16 nm and the length was up to 800 nm, while the average diameters for G-180 increased up to about 26 nm. The diameters of the nanorods obtained by TEM measurements were slightly larger than the calculated values from (110) diffraction peak using Scherrer formula, which might be related to the presence of non-crystalline surface layers [16]. The average particle sizes calculated from the diffraction peak (110) reflected the diameters of the nanorods approximately. Therefore, in the following discussion, we would use the average particle sizes calculated from diffraction peak (110) to address the diameter effect of nanorods.

Specific surface areas of the goethite nanorods were determined using BET technique. Figure 3 shows the BET surface areas for all samples as a function of the rod diameter. The specific surface areas of goethite nanorods decreased with increasing the rod diameter. The relationship between the BET surface area values (*S*) and the rod diameters (*D*) can be described by a simple function: $S= -10+942/D$. If the goethite nanorods are approximately taken as a column form, the specific surface areas can be expressed as: $S=\pi DL/\pi(D/2)^2L\rho=(4/\rho)(1/D)$, where *L* is the length of the nanorod, ρ is the density of the goethite. Assuming that the density of the present nanorods equals to $\rho=4.258$ g cm^{-3} for bulk goethite, we obtained constant term of $4/\rho=939.4$ (m^2 g^{-1}nm) very close to 942 (m^2 g^{-1}nm). This means that the goethite nanorods were well dispersed with a weak agglomeration.

Goethite structure is characterized by relatively dense packing and strong hydrogen bonding with iron ions that occupy one-half of the vacancies in an approximately hexagonally closely packed oxygen framework [17]. All hydroxyl units are in the same environments, while the hydrogen bonds point in two different directions [18]. The splitting of the hydroxyl stretching and deformation bands are the result of the strong coupling between the different hydroxyl modes [18]. Figure 4 shows the infrared spectra of the hydrated goethite nanorods. A very strong band observed at about 3135 cm^{-1} is associated with the typical bulk hydroxyl stretching mode in goethite, whereas the weak shoulder near 3415 cm^{-1} is ascribed to the stretching modes of the surface absorbed water. With increasing the treatment temperatures (also the rod diameters), the intensity of the band at 3415 cm^{-1} gradually reduced, indicating a decrease in the hydration content, which is further confirmed by our TG. In the range of 400–1000 cm^{-1}, four strong bands located at 898 (ν_1), 797 (ν_2), 631 (ν_3) and 459 (ν_4) cm^{-1} with two weak shoulder vibrations near 670 and 490 cm^{-1} were observed. The band near 898 cm^{-1} (ν_1) is attributed to the hydroxyl deforma-

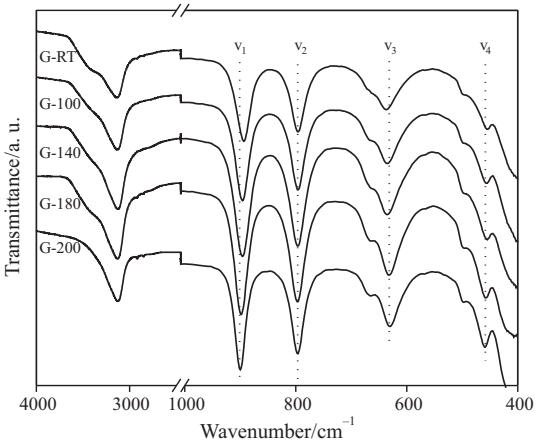

Fig. 4 FTIR spectra of goethite nanorods

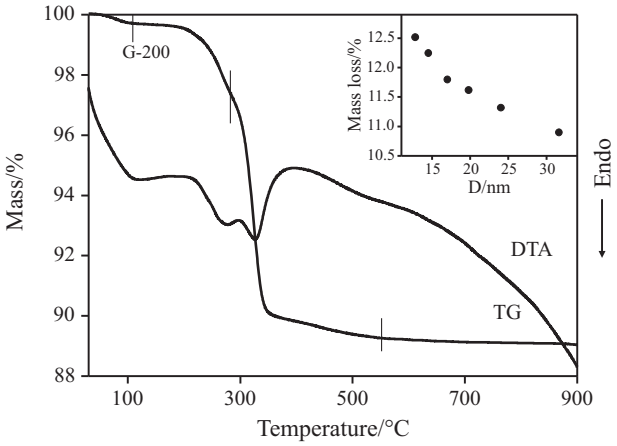

Fig. 5 TG-DTA curves of sample G-200. Inset shows the variation of total mass loss via the average diameters of goethite nanorods

tion vibration in the *a*–*b* plane, and the band at about 797 cm^{-1} (ν_2) is ascribed to the hydroxyl deformation vibration that is parallel to the *c*-axis. These bands are diagnostic bands of goethite [17]. Applying a method of normal coordinate analysis, Verdonck *et al*. [14] calculated the vibrational frequencies for goethite and deuterated goethite and found that the infrared bands at 630 and 495 cm^{-1} were rather insensitive to deuteration and assigned to Fe–O stretching vibrations. Therefore, the band observed at 631 cm^{-1} (ν_3) in Fig. 4 can be ascribed to Fe–O vibration in *a*–*b* plane, while the 459 cm^{-1} (ν_4) band is attributed to Fe–O vibration in *b*–*c* plane [18]. It is noted from Fig. 4 that both bands ν_1 and ν_4 shifted towards higher frequencies, while the band ν_3 to lower frequency as rod diameters increased. Band ν_2 almost kept the constant frequency. The blue shift of ν_1 band is indicative of an increased strength of O–H bond, which will be further discussed in terms of the TG analysis. As stated above, the as-obtained goethite nanorods were oriented along *c*-axis direction. The band ν_2 located at about 797 cm^{-1} is originated from the hydroxyl deformation vibration parallel to *c*-axis. Therefore, no obvious shift was observed for ν_2. On the other hand, the red shift of ν_3 band might be related to the enhanced ionicity of Fe–O bond in the *a*–*b* plane and the increased crystallinity [19].

The surface hydration structure and thermal stability properties of goethite samples were examined by TG-DTA. A typical TG-DTA profile for G-200 is presented in Fig. 5. The curves of other goethite samples (not shown) exhibited similar thermal behaviors to that of G-200. Contrast to the continuous mass loss reported in [20], three well-resolved mass loss steps were observed in the temperature range of 30–700°C, and the corresponding endothermic peaks in DTA curve were also seen at about 105, 270, and 315°C, respectively. Above 550°C, sample mass remained constant. The total mass loss is about 11% for G-200, which is slightly larger than the theoretical value of 10.1% for FeOOH. The extra mass loss should come from the absorbed water. Furthermore, the total mass loss monotonously increased as the specific surface areas (or reduction of the rod diameters), as shown in inset of Fig. 5, which is in good agreement with our FTIR spectral observation.

For our goethite nanorods, the first mass loss step occurring at about 105°C is mainly assigned to the removal of free water or physisorbed water. It has been often reported that the mass loss in the temperature range from 200 to 700°C with an endothermic peak corresponds to the dehydroxylation of goethite [20]. However, in the same temperature range, the mass loss for our goethite nanorods took place in two discrete steps with a double endothermic peak. The differential thermogravimetry (DTG) curves clearly showed these discrete processes, as illustrated in Fig. 6. It is worthy to note that peak temperatures of DTG are identical to the corresponding temperatures in DTA curves. With increasing the rod diameter, the intensity of the DTG peaks at about 100°C became weaker, indicating the decrease of physisorbed water. On the other hand, accompanying the decrease in relative intensity of peak at about 270°C, rod diameter increase also moved the DTG peak at about 300°C to high temperatures.

Concerning the dehydration reaction, Ishikawa *et al.* [21] observed several endothermic peaks for Ti-doped α-FeOOH particles in the temperature from 200 to 300°C. They thought that the number of dehydroxylation endothermic peaks was related to the crystallinity of goethite samples. Schwertmann [22] reported a double peak of dehydroxylation for well crystallized α-FeOOH and attributed it to an intermediate phase with a slightly higher dehydroxylation temperature generated during heating. Al-substituted goethite was also found to show a double peak, which was ascribed to the difference of dehydroxylation temperatures of Al–OH and Fe–OH [23]. In order to explore the ori-

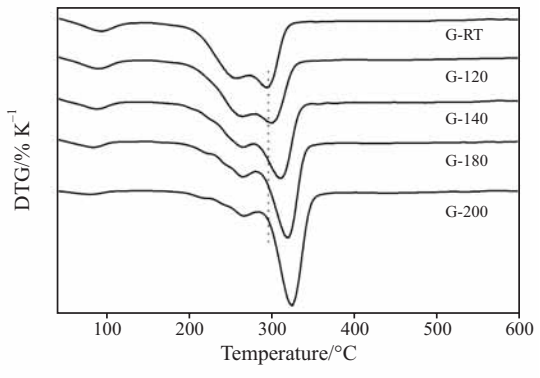

Fig. 6 DTG curves of goethite nanorods

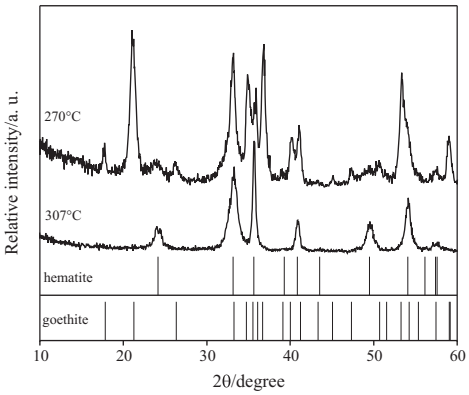

Fig. 7 X-ray diffraction patterns of the dehydroxylated products of G-RT sample quenched at 270°C and 307°C. Vertical bars represent the standard diffraction data from JCPDS files for bulk goethite (No. 29-0713) and hematite (No. 33-664)

gin of the double mass loss steps in the temperature range of 250–350°C and get some insights into the mechanism of dehydration of goethite, the products were quenched from 270 and 370°C during heating the sample G-RT in TG-DTA measurement. Their XRD patterns are shown in Fig. 7. It can be seen that the product quenched from 270°C remained a tetragonal α-FeOOH phase coexisting with a minor part of α-Fe_2O_3, while no traces of hydrohematite or other intermediate [24] were observed. With increasing the temperature up to 307°C, goethite completely transformed into α-Fe_2O_3. Therefore, the double peaks should be associated with different chemical processes.

For the goethite nanorods, there might exist ample dangling bonds at the surfaces due to the unsaturated coordination of Fe atom. These dangling bonds would interact with the water molecules on surfaces, resulting in the hydrated surface structure. Therefore, the surface hydrated structure could be stabilized by the hydrogen bonds with the coordinated oxygen of goethite lattice and the adjacent bridging OH^- groups. One or two atomic layers of water molecules (referred as chemisorbed water) formed a stable hydrated termination of the goethite nanorods, as confirmed by the outmost amorphous layers of nanorods in Figs 2c and d. These stable hydrated termination layers would be firstly removed when the temperature was increased to 206°C, and a skin of α-Fe_2O_3 shell would form in the surface of goethite to retard the dehydration of the bulk [24]. Therefore, the second mass loss step, corresponding to the DTG peak at about 270°C primarily originates from the dehydration of chemisorbed water or the amorphous layers of nanorods. The thermal stability of the amorphous layers is independent on the diameters of the goethite nanorods. As indicated in Fig. 6, the temperatures of the second maximal mass loss peak kept nearly constant for all goethite nanorods. Further increasing temperature led to a complete dehydration of goethite nanorods and transformation into hematite. The third and most important region of mass loss with a corresponding endothermic peak at 315°C is associated with the dehydration of bulk structural hydroxyl and conversion of goethite to hematite. Comparing the preciously reported dehydration temperatures [18], our goethite samples showed higher dehydration temperature because the hydrated surface structure can hinder the dehydroxylation. On the other hand, with increasing the rod diameter, the positions of the mass loss peaks associated with the dehydroxylation of bulk structural hydroxyl shifted toward higher temperatures, which should be related to the variation of strength for Fe–O–H bonds, similar to many other particle size-induced structural transformations [25].

Goethite is a main component of soil clay minerals [26], and could act as the dominant adsorbent in removing the heavy metal ions from wastewater. It is presumed that adsorption involves both a coordination interaction at specific surface sites of goethite and electrostatic interaction between adsorbing ions and the charged surfaces [27], which is dominated by the surface structural properties of goethite. For the heavy metal contamination, three most detrimental metals are cadmium, mercury, and lead. Cadmium has the most dangerous long-term effects on human health [28]. Therefore, the adsorption property of as-obtained goethite nanorods in removing heavy metal ions was evaluated by selecting cadmium ions as the contamination species to remove. The effect of cadmium removal with G-140 as the contact time is shown in Fig. 8. Inset Fig. 8 shows the percentage uptake of Cd^{2+} on goethite nanorods with different specific surface areas for 5 and 120 min. It appears that for a relatively short time period, significant removal of Cd^{2+} ions is achieved. After this initial fast adsorption period, the uptake of Cd^{2+} ions reaches the adsorption equilibrium in about 60 min and the maximum adsorption percentage is 96.4%. The ability of cadmium removal increased with the surface areas of

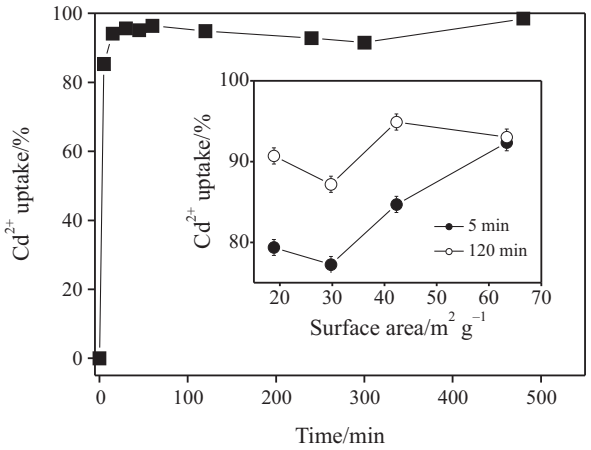

Fig. 8 Adsorption of Cd^{2+} ions onto G-140 as a function of contact time. The inset is the variation Cd^{2+} uptake with surface area in 5 and 120 min

goethite nanorods. It is noted that the maximum adsorption decreased only slightly with time till 300 min and again slightly increased with time. Furthermore, all of the adsorptions remained above 91%, suggesting that the goethite nanorods possessed an excellent removal capacity of Cd^{2+} ions from aqueous solution. The detailed investigation of removal of other heavy metal ions by goethite nanorods is under progress.

Conclusions

Goethite nanorods with different diameters were prepared via a simple hydrothermal method. The hydroxyl deformation vibration in *a–b* plane showed a blue shift with increasing the rod diameter, indicating the increased strength of O–H bond. The opposite shift of Fe–O vibration observed in *a–b* plane is associated with the decreased covalency of Fe–O. All goethite nanorods contained a hydrated amorphous layer on their surface, which decomposed at 270°C regardless of the rod diameter and formed a skin of α-Fe_2O_3 shell in the surface of goethite to retard the dehydration of the bulk. Further increasing beyond 300°C led to a complete dehydration of goethite nanorods and transformation into hematite. The as-prepared goethite nanorods are proved to be promising in removal of Cd^{2+} ions from wastewater.

Acknowledgements

This work was financially supported by NSFC under the contract (No. 20671092), a grant from Hundreds Youth Talents Program of CAS (Li G.), and in part by a Science and Technology Program from Fujian Province (No. 2006J0178), and National Basic Research Program of China (973 Program, No. 2007CB613306).

References

1 J. L. Jambor and J. E. Dutrizac, Chem. Rev., 98 (1998) 2549.
2 M. Ponthieu, F. Juillot, T. Hiemstra, W. H. van Riemsdijk and M. F. Benedetti, Geochim. Cosmochim. Acta, 70 (2006) 2679.
3 C. Sikalidis, T. Zorba, K. Chrissafis, K. M. Paraskevopoulos and K. M. Paraskevopoulos, J. Therm. Anal. Cal., 86 (2006) 411.
4 D. Walter, G. Buxbaum and W. Laqua, J. Therm. Anal. Cal., 63 (2001) 733.
5 E .Wolska, Solid State Ionics, 28–30 (1988) 1349.
6 Ö. Özdemir and D. J. Dunlop, Earth Planet. Sci. Lett., 177 (2000) 59.
7 A. F. Gualtieri and P. Venturelli, Am. Mineral., 84 (1999) 895.
8 F. Watari, P. Delavignette, J. Van Landuty and S. Amelinckx, J. Solid State Chem., 48 (1983) 49.
9 C. J. Goss, Miner. Mag., 51 (1987) 437.
10 A. Navrotsky, Proc. Natl. Acad. Sci. U. S. A., 101 (2004) 12096.
11 J. D. Betancur, C. A. Barrero, J. M. Greneche and G. F. Goya, J. Alloys Compd., 369 (2004) 247.
12 L. Lu, L. P. Li, X. J. Wang and G. S. Li, J. Phys. Chem. B, 109 (2005) 17151.
13 G. S. Li, L. P. Li, J. Boerio-Goates and B. F. Woodfield, J. Am. Chem. Soc., 127 (2005) 8659.
14 L. Verdonck, S. Hoste, F. F. Roelandt and G. P. Van Der Kelen, J. Mol. Struct., 79 (1982) 273.
15 H. D. Ruan, R. L. Frost, J. T. Kloprogge and L. Duong, Spectrochim. Acta, Part A, 58 (2002) 479.
16 J. Joo, S. J. Lee, D. H. Park, Y. S. Kim, Y. Lee, C. J. Lee and S. R. Lee, Nanotechnology, 17 (2006) 3506.
17 Q. Williams and L. Guenther, Solid State Commun., 100 (1996) 105.
18 H. D. Ruan, R. L. Frost and J. T. Kloprogge, Spectrochim. Acta, Part A, 5 (2001) 2575.
19 S. Krehula, S. Popovic and S. Music, Mater. Lett., 54 (2002) 108.
20 H. L. Fan, B. Z. Song, J. H. Liu, Z. Q. Yang and Q. X. Li, Mater. Chem. Phys., 89 (2005) 321.
21 T. Ishikawa, H. Yamashita, A. Yasukawa, K. Kandori, T. Nakayama and F. Yuse, J. Mater. Chem., 10 (2000) 543.
22 U. Schwertmann, Thermochim. Acta, 78 (1984) 39.
23 M. V. Fey and J. B. Dixon, Clays Clay Miner., 29 (1981) 91.
24 R. Derie, M. Ghodsi and C. Calvo-Roche, J. Thermal Anal., 9 (1976) 435.
25 S. Tsunekawa, K. Ishikawa, Z. Q. Li, Y. Kawazoe and A. Kasuya, Phys. Rev. Lett., 85 (2000) 3440.
26 M. Laskou, G. Margomenou-Leonidopoulou and V. Balek, J. Therm. Anal. Cal., 84 (2006) 141.
27 T. Hiemstra and W. H. Van Riemsdijk, J. Colloid Interface Sci., 179 (1996) 488.
28 A. Demirbas, J. Hazard. Mater., 109 (2004) 221.

Received: May 30, 2007
Accepted: July 31, 2007

DOI: 10.1007/s10973-007-8575-9